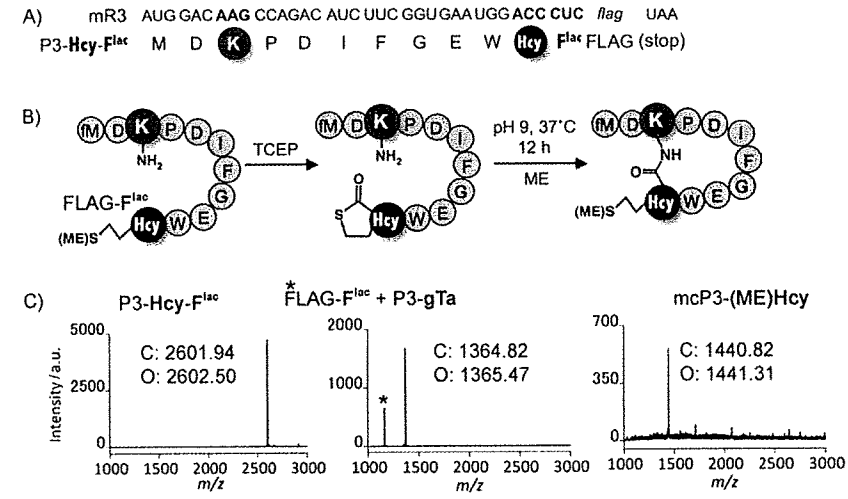

Figure 4. Macrocyclization of P3 with γ-thiolactone. A) Sequences of mR3 and P3-Xaa-F^{lac}. (ME)Hcy and F^{lac} are assigned to codons ACC and CUC, respectively. B) Schematic representation of the macrocyclization with P3-gTa. TCEP reduction of P3-Hcy-F^{lac} induced the formation of P3-gTa, which was incubated with ME (10 mM) at pH 9.0, 37 °C for 12 h. These procedures afforded mcP3-(ME)Hcy through linkage between the C terminus and the side chain of the K residue. C) MALDI-TOF analysis of the corresponding peptides. Calculated (C) and observed (O) molecular masses for the singly charged species, $[M+H]^+$, of the peptide are shown in each spectrum. The asterisk (*) denotes a peak corresponding to liberated F^{lac}-FLAG from P3-Hcy-F^{lac}; calcd: 1162.13, found: 1163.44.

the immobilized peptide was eluted with TFA (0.2%, 5 μL). The resulting peptide was desalted with a C18 micro-ZipTip (Millipore), and eluted with aq. acetonitrile (50%, 1 μL, 0.1% TFA), saturated with the matrix (*R*)-cyano-4-hydroxycinnamic acid. Mass measurements were performed by MALDI-TOF (autoflex TOF/TOF, Bruker).

Synthesis of C-terminal γ/δ-lactams or thiolactones: For the C-terminally cyclized peptides, translation product (5 μL) was mixed with TCEP (100 mM, 0.5 μL) and bicine-KOH (1 M, pH 9.0, 0.5 μL) at room temperature for 2 h. For the confirmation of cyclization, the mixture was purified on FLAG resin, eluted with TFA (0.2%, 5 μL), and analyzed by MALDI-TOF.

C-terminal modification with various alkylamides: For C-terminal modification with various alkylamides, the C-terminal γ-thiolactone peptide was prepared as described above, in 5 μL total volume. The mixture was incubated with alkylamine (2 M, 0.5 μL, ammonia, isobutylamine, cyclopentylamine, allylamine, propargylamine, 3-ethoxypropylamine, octylamine, nonylamine, geranylamine, benzylamine, pyridoxine, 4-aminobutanoic acid, or dansylcadaverine, as shown in Figure 3B) at 25°C for 2 h. These alkylamines were purchased from Kanto Chemicals (Tokyo, Japan), Sigma–Aldrich (Japan), or Nacalai Tesque (Kyoto, Japan). For the confirmation of modification, the mixture was purified on FLAG resin, eluted with TFA (0.2%, 2 μL), and analyzed by MALDI-TOF. Note that ME (1 mM) was included in the *w*PURE system as one of the standard reagents, and occasionally formed a disulfide bond with the free sulfhydryl group in residues such as Hcy and Cys by air oxidation.

Peptide macrocyclization: For the macrocyclization of the peptide, the C-terminal γ-thiolactone peptide was synthesized as described above in a total volume of 5 μL, and purified on FLAG resin and eluted with TFA (0.2%, 5 μL). The eluent was incubated with 2-mercaptoethanol (100 mM, 0.5 μL) and bicine-KOH (1 M, pH 9.0, 0.5 μL) at 37 °C for 12 h to induce the macrocyclization between the C terminus and the lysine side chain.

Acknowledgements

This work was supported by Technology Program grants from the New Energy and Industrial Technology Development Organization (NEDO) and the Japan Society for the Promotion of Science Grants-in-Aid for Scientific Research (S) (16101007) to H.S., and from the Global COE Program "Chemistry Innovation through Cooperation of Science and Engineering", MEXT, Japan to E.N.

Keywords: genetic code · peptidomimics · protein engineering · ribosomal synthesis · ribozymes

[1] L. L. Kisselev, R. H. Buckingham, *Trends Biochem. Sci.* **2000**, *25*, 561.
[2] S. Petry, A. Weixlbaumer, V. Ramakrishnan, *Curr. Opin. Struct. Biol.* **2008**, *18*, 70.
[3] D. J. Merkler, *Enzyme Microb. Technol.* **1994**, *16*, 450.
[4] A.-J. Ren, Z.-F. Guo, Y.-K. Wang, L. Lin, X. Zheng, W.-J. Yuan, *Peptides* **2009**, *30*, 439.
[5] V. Sanchez-Margalet, M. Lucas, R. Goberna, *J. Mol. Endocrinol.* **1996**, *16*, 1.
[6] L. Hilsted, K. Hint, J. Christiansen, J. F. Rehfeld, *Gastroenterology* **1988**, *94*, 96.
[7] K. R. Shoemaker, P. S. Kim, D. N. Brems, S. Marqusee, E. J. York, I. M. Chaiken, J. M. Stewart, R. L. Baldwin, *Proc. Natl. Acad. Sci. USA* **1985**, *82*, 2349.
[8] A. Wettergren, L. Pridal, M. Wojdemann, J. J. Holst, *Regul. Pept.* **1998**, *77*, 83.
[9] A. F. Bradbury, D. G. Smyth, *Biosci. Rep.* **1987**, *7*, 907.
[10] I. R. Cottingham, A. Millar, E. Emslie, A. Colman, A. E. Schnieke, C. McKee, *Nat. Biotechnol.* **2001**, *19*, 974.
[11] T. J. Tolbert, C.-H. Wong, *J. Am. Chem. Soc.* **2000**, *122*, 5421.
[12] J. Mukhopadhyay, A. N. Kapanidis, V. Mekler, E. Kortkhonjia, Y. W. Ebright, R. H. Ebright, *Cell* **2001**, *106*, 453.
[13] B. Zhang, Z. Tan, L. G. Dickson, M. N. Nalam, V. W. Cornish, A. C. Forster, *J. Am. Chem. Soc.* **2007**, *129*, 11316.
[14] Z. Tan, A. C. Forster, S. C. Blacklow, V. W. Cornish, *J. Am. Chem. Soc.* **2004**, *126*, 12752.
[15] Z. Tan, S. C. Blacklow, V. W. Cornish, A. C. Forster, *Methods* **2005**, *36*, 279.
[16] A. O. Subtelny, M. C. Hartman, J. W. Szostak, *J. Am. Chem. Soc.* **2008**, *130*, 6131.
[17] C. Merryman, R. Green, *Chem. Biol.* **2004**, *11*, 575.
[18] K. Josephson, M. C. Hartman, J. W. Szostak, *J. Am. Chem. Soc.* **2005**, *127*, 11727.
[19] M. C. Hartman, K. Josephson, C. W. Lin, J. W. Szostak, *PLoS ONE* **2007**, *2*, e972.
[20] A. Frankel, S. W. Millward, R. W. Roberts, *Chem. Biol.* **2003**, *10*, 1043.
[21] A. C. Forster, H. Weissbach, S. C. Blacklow, *Anal. Biochem.* **2001**, *297*, 60.
[22] A. C. Forster, Z. Tan, M. N. Nalam, H. Lin, H. Qu, V. W. Cornish, S. C. Blacklow, *Proc. Natl. Acad. Sci. USA* **2003**, *100*, 6353.
[23] Y. Shimizu, Y. Kuruma, B. W. Ying, S. Umekage, T. Ueda, *FEBS J.* **2006**, *273*, 4133.
[24] Y. Shimizu, T. Kanamori, T. Ueda, *Methods* **2005**, *36*, 299.
[25] Y. Shimizu, A. Inoue, Y. Tomari, T. Suzuki, T. Yokogawa, K. Nishikawa, T. Ueda, *Nat. Biotechnol.* **2001**, *19*, 751.

[26] H. Murakami, A. Ohta, H. Ashigai, H. Suga, *Nat. Methods* **2006**, *3*, 357.
[27] A. Ohta, H. Murakami, E. Higashimura, H. Suga, *Chem. Biol.* **2007**, *14*, 1315.
[28] Y. Goto, H. Murakami, H. Suga, *RNA* **2008**, *14*, 1390.
[29] Y. Goto, A. Ohta, Y. Sako, Y. Yamagishi, H. Murakami, H. Suga, *ACS Chem. Biol.* **2008**, *3*, 120.
[30] T. J. Kang, H. Suga, *Biochem. Cell Biol.* **2008**, *86*, 92.
[31] T. J. Kang, S. Yuzawa, H. Suga, *Chem. Biol.* **2008**, *15*, 1166.
[32] T. Kawakami, H. Murakami, H. Suga, *J. Am. Chem. Soc.* **2008**, *130*, 16861.
[33] A. Ohta, H. Murakami, H. Suga, *ChemBioChem* **2008**, *9*, 2773.
[34] Y. Sako, Y. Goto, H. Murakami, H. Suga, *ACS Chem. Biol.* **2008**, *3*, 241.
[35] Y. Sako, J. Morimoto, H. Murakami, H. Suga, *J. Am. Chem. Soc.* **2008**, *130*, 7232.
[36] T. Kawakami, H. Murakami, H. Suga, *Chem. Biol.* **2008**, *15*, 32.
[37] L. Cartwright, D. W. Hutchinson, V. W. Armstrong, *Nucleic Acids Res.* **1976**, *3*, 2331.
[38] C. E. Hop, R. Bakhtiar, *Rapid Commun. Mass Spectrom.* **2002**, *16*, 1049.
[39] J. Perła-Kaján, T. Twardowski, H. Jakubowski, *Amino Acids* **2007**, *32*, 561.

Received: February 4, 2009
Published online on April 15, 2009

J|A|C|S COMMUNICATIONS

Published on Web 03/20/2009

Translation Initiation with Initiator tRNA Charged with Exotic Peptides

Yuki Goto[†,‡] and Hiroaki Suga[*,†,‡]

Research Center for Advanced Science and Technology and Department of Advanced Interdisciplinary Studies, The University of Tokyo, 4-6-1, Komaba, Meguro-ku, Tokyo 153-8904, Japan

Received January 24, 2009; E-mail: hsuga@rcast.u-tokyo.ac.jp

The translation system evolved to polymerize 20 specific kinds of proteinogenic L-α-amino acids with extremely high accuracy according to the sequence information encoded in mRNA. Exclusion of nonproteinogenic amino acids from the polymerization is achieved by sophisticated mechanisms involving the multistep selection of correctly charged aminoacyl-tRNAs.[1] Despite the fact that techniques allowing researchers to manipulate the genetic code, so-called genetic code expansion[2] or genetic code reprogramming,[3] have been developed and many successes in incorporating non-proteinogenic L-α-amino acids into nascent peptide chain have been reported, nonproteinogenic amino acids containing more drastically altered structures (referred to as exotic amino acids), such as D- and β-amino acids, are notoriously difficult or often impossible to be elongated.[2a−c,3c,4] On the other hand, recent investigations have shown that the initiation apparatus is more tolerant to exotic amino acids than elongation event. In fact, it has been reported that "nonmethionine" amino acids, for example, various L-α-amino acids[5a] and some D-α-amino acids[5b] with or without *N*-acyl groups, were able to initiate translation, whereas formylmethionine (fMet) is a sole initiator in the ordinary prokaryotic translation system (Figure 1A).[6] The observed tolerance of initiation has prompted

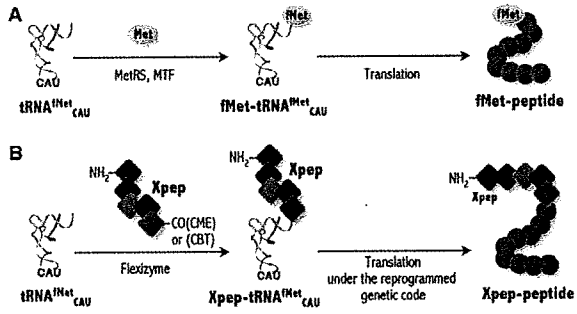

Figure 1. Reprogramming of the initiation event with exotic peptides. (A) Initiation in an ordinary prokaryotic translation system. The initiator tRNA (tRNA$^{fMet}_{CAU}$) is methionylated by methionyl-tRNA synthetase (MetRS) and its α-amino group is formylated by methionyl-tRNA formyltransferase (MTF) to afford fMet-tRNA$^{fMet}_{CAU}$. Initiation with fMet-tRNA$^{fMet}_{CAU}$ yields a peptide containing fMet at the N-terminus (fMet-peptide). (B) Outline of translation initiation with exotic peptides reported here. Flexizyme charges a short exotic peptide (Xpep) onto the tRNA$^{fMet}_{CAU}$. Reprogramming of the initiation event allows us to prime the translation reaction with Xpep-tRNA$^{fMet}_{CAU}$, yielding a peptide bearing several exotic amino acids at the N-terminus (Xpep-peptide).

us to further explore the repertoire expansion. Here we report the reprogramming of translation initiation with "exotic peptides" containing several exotic amino acids (Figure 1B).

To facilitate the reprogramming of initiation event, we utilized our original methodology in the combination of flexizyme and *w*PURE systems. The former system consists of a tRNA aminoacylation ribozyme, referred to as flexizyme, enabling us to charge a wide variety of nonproteinogenic amino acids activated with certain ester or thioester groups onto the 3′ hydroxyl group of any desired tRNAs, including the initiator tRNA$^{fMet}_{CAU}$.[3c] The latter system is based on a reconstituted *E. coli* cell-free translation system, so-called protein-translation using recombinant elements (PURE),[7] in which methionine (Met) is *withdrawn* to make the start codon vacant and thus it is called a *w*PURE system.[5,8] By using the integrated systems, that is, by adding an acylated tRNA$^{fMet}_{CAU}$ prepared by flexizyme to the *w*PURE system, the start codon AUG was reassigned from fMet to desirable non-fMet initiators.[5]

Although the flexizyme system has provided us a nearly unlimited opportunity for the synthesis of tRNA charged with nonproteinogenic amino acids (Xaa-tRNA),[3c,5,8] it is unknown if it can be applicable to tRNA peptidylation. We therefore first verified whether exotic peptides (Xpep) could be charged onto tRNA$^{fMet}_{CAU}$ by means of flexizyme. We designed eleven short peptides containing various combinations of proteinogenic amino acids and exotic amino acids including D-phenylalanine (^{D}Phe), D-glutamic acid (^{D}Glu), D-lysine (^{D}Lys), *N*-methyl-L-phenylalanine (^{Me}Phe), *N*-methyl-L-glutamic acid (^{Me}Glu), 4-aminobenzoic acid (^{4}Abz) and β-alanine (βAla) (the individual structures are shown in Supporting Information, Figure S1). To make the peptides to be accessible to the flexizyme system, those containing the C-terminal ^{L}Phe, ^{D}Phe, ^{Me}Phe, or ^{L}Met were derived to the cyanomethyl esters (CME) (Table 1, entries 1−8, 10, and 11), while one containing the C-terminal ^{L}Gln was derived to 4-cholorobenzyl thioester (CBT)

Table 1. The Sequences of Peptide Initiators Used in This Study and Their Acylation Yields and Translation Efficiencies

entry	initiator sequence[a]	activating group for flexizyme[b]	acylation yield (%)[c]	translation efficiency (%)[d]
1	^{D}Phe−^{L}Phe	CME	85	88
2	^{D}Phe−^{D}Phe−^{L}Phe	CME	44	68
3	^{D}Phe−^{4}Abz−^{L}Phe	CME	30	133
4	^{D}Phe−βAla−^{L}Phe	CME	69	115
5	^{D}Phe−^{Me}Glu−^{L}Phe	CME	47	39
6	^{D}Phe−βAla−^{D}Phe	CME	68	26
7	^{D}Phe−βAla−^{Me}Phe	CME	66	88
8	^{D}Phe−βAla−^{L}Met	CME	48	91
9	^{D}Phe−βAla−^{L}Gln	CBT	38	19
10	^{D}Glu−^{D}Lys−^{L}Phe	CME	55	25
11	^{D}Glu−^{D}Lys−^{D}Glu−^{D}Lys−^{L}Phe	CME	55	12

[a] ^{D}Xaa, ^{L}Xaa, ^{Me}Xaa, ^{4}Abz, and βAla denote D-amino acids, L-amino acids, *N*-methyl-*L*-amino acids, 4-aminobenzoic acid, and β-alanine, respectively. [b] CME and CBT denote cyanomethyl ester and 4-chlorobenzyl thioester activating groups, respectively. [c] Yields of the acylation were calculated based on the band intensity in acid PAGE (see Figure S2 for the detailed description). [d] Relative translation efficiencies of Xpep-peptides were determined by comparing with the band intensity of fMet-peptide in tricine-SDS PAGE (see Figure 2B). The expression quantity of the fMet-peptide was determined to be 7.5 pmol/μL based on the method reported elsewhere.[5a,8b]

† Research Center for Advanced Science and Technology.
‡ Department of Advanced Interdisciplinary Studies.

10.1021/ja900597d CCC: $40.75

(Table 1, entry 9). For verification of the peptidylation ability of flexizyme, we used our conventional assay system using a tRNA analogue, microhelix RNA.[3c] The di-, tri-, and pentapeptide substrates were incubated with the microhelix RNA in the presence of the flexizyme, and the products were analyzed by denaturing acid polyacrylamide gel electrophoresis (PAGE). In all cases, a single mobility-shifted band corresponding to the individual Xpep-RNA was observed (Figure S2), indicating that the flexizyme system is compatible to the peptidyl substrates for tRNA peptidylation. Importantly, the observed yields were in the range of 30−69% (Table 1), which were sufficient to carry out the translation experiment based on our previous experimental knowledge.[3c] We thus next investigated whether the translation apparatus could accept these Xpep-tRNA$^{fMet}_{CAU}$ as an initiator.

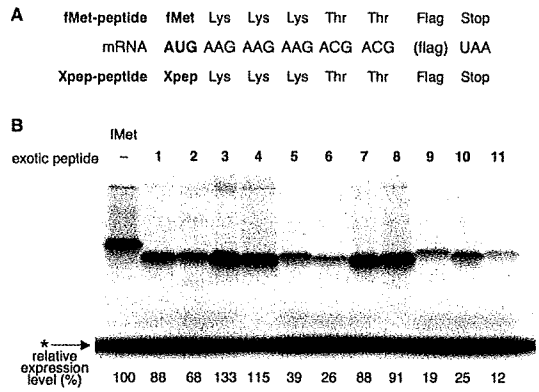

Figure 2. Translation initiation with exotic peptides. (A) Sequences of a mRNA template and expressed fMet/Xpep-peptides. Flag in the parentheses indicates the RNA sequence encoding a Flag peptide (DYKDDDDK). (B) Tricine-SDS PAGE of the translation products initiated with various exotic peptides. The product of the *w*PURE translation reaction containing each Xpep-tRNA$^{fMet}_{CAU}$ and [^{14}C]-Asp was analyzed by tricine-SDS PAGE (lanes 1−11 corresponding the exotic peptides shown in Figure S1). "fMet" indicates the wild-type expression in the ordinary PURE system in which fMet acted as the initiator. Each expression level relative to the fMet-peptide is determined by a mean score of triplicates or more. The band indicated by the asterisk corresponds to the remaining [^{14}C]-Asp that was not incorporated into the peptide.

We designed a mRNA template that encoded a 14-mer peptide, in which the C-terminus contained a Flag peptide sequence for the convenience of radiolabeling-detection using [^{14}C]-Asp as well as the peptide isolation (Figure 2A). Each peptide was expressed in the presence of the respective Xpep-tRNA$^{fMet}_{CAU}$ in the *w*PURE system, where the initiator was reassigned to the short exotic peptide. The translation product was analyzed by tricine-SDS PAGE (Figure 2B) and its relative translation efficiency was determined by the comparison with the wild-type expression where fMet acted as the initiator in the ordinary PURE system (Table 1). In addition, the expressed peptide was subjected to mass spectrometry for identification of the translation product (Figure S3). To our surprise, all Xpep-tRNAs could initiate the translation. The expression efficiencies were depending upon the peptides, ranging from 12% to 133% relative to the fMet-peptide expression. Although we could not define a general trend that correlated the sequence compositions to the observed expression levels, the longest peptide **11** was least efficient so that the long length of peptide might hamper the initiation event. Given the lower efficiency in relatively hydrophilic peptides (**5**, **9**, **10**, and **11**) and the previous observation that hydrophilic amino acids could initiate translation less efficiently than hydrophobic ones,[5] the hydrophilicity of initiator might also affect the initiation efficiency. Nonetheless, it is clear that exotic peptides containing consecutive D-amino acids or the combination of exotic amino acids charged onto tRNA$^{fMet}_{CAU}$ could initiate the translation to afford peptides containing a stretch of exotic amino acids at the N-terminus.

Here we have reported that ribosome is able to accept tRNA$^{fMet}_{CAU}$charged with nonstandard peptides as an initiator, and thus peptides containing a variety of exotic amino acids at the N-terminus could be expressed. To the best of our knowledge, this work represents the first demonstration of translation initiation with peptidyl molecules regardless of natural or non-natural building blocks. In contrast to the fact that elongation of exotic amino acids has often encountered difficulties, the initiation reprogramming approach enables us to synthesize peptides containing exotic amino acids at the N-terminus. Particularly, we envisage that the integration of this approach with appropriate peptide cyclization techniques[5a,8c] will open a new avenue for the ribosomal synthesis of unusual peptides. Moreover, the reported method facilitating the synthesis of desired peptidyl-tRNAs with proteinogenic or exotic amino acids by means of flexizyme system would provide a new tool for studying the mechanism of initiation and/or elongation in translation.

Acknowledgment. We thank Dr. Hiroshi Murakami for valuable discussion and suggestion. We thank Professor Kazuhiko Nakatani for the use of ESI-TOF instrumentation. We also thank Mr. Yusuke Yamagishi for assistance with manuscript preparation. This work was supported by grants of Japan Society for the Promotion of Science Grants-in-Aid for Scientific Research (S) (16101007) to H.S., Grants-in-Aid for JSPS Fellows (18-10526) to Y.G., and a research and development projects of the Industrial Science and Technology Program in the New Energy and Industrial Technology Development Organization (NEDO).

Supporting Information Available: Detailed structure of short peptides used here, acid PAGE analysis, mass spectra, and experimental methods. This material is available free of charge via the Internet at http://pubs.acs.org.

References

(1) (a) Söll, D. *Experientia* **1990**, *46*, 1089–1096. (b) Sankaranarayanan, R.; Moras, D. *Acta Biochim. Pol.* **2001**, *48*, 323–335.
(2) (a) Roesser, J. R.; Xu, C.; Payne, R. C.; Surratt, C. K.; Hecht, S. M. *Biochemistry* **1989**, *28*, 5185–5195. (b) Bain, J. D.; Diala, E. S.; Glabe, C. G.; Wacker, D. A.; Lyttle, M. H.; Dix, T. A.; Chamberlin, A. R. *Biochemistry* **1991**, *30*, 5411–5421. (c) Ellman, J. A.; Mendel, D.; Schultz, P. G. *Science* **1992**, *255*, 197–200. (d) Link, A. J.; Mock, M. L.; Tirrell, D. A. *Curr. Opin. Biotechnol.* **2003**, *14*, 603–609. (e) Wang, L.; Xie, J.; Schultz, P. G. *Annu. Rev. Biophys. Biomol. Struct.* **2006**, *35*, 225–249.
(3) (a) Forster, A. C.; Tan, Z.; Nalam, M. N.; Lin, H.; Qu, H.; Cornish, V. W.; Blacklow, S. C. *Proc. Natl. Acad. Sci. U.S.A.* **2003**, *100*, 6353–6357. (b) Josephson, K.; Hartman, M. C.; Szostak, J. W. *J. Am. Chem. Soc.* **2005**, *127*, 11727–11735. (c) Murakami, H.; Ohta, A.; Ashigai, H.; Suga, H. *Nat. Methods* **2006**, *3*, 357–359.
(4) (a) Starck, S. R.; Qi, X.; Olsen, B. N.; Roberts, R. W. *J. Am. Chem. Soc.* **2003**, *125*, 8090–8091. (b) Tan, Z.; Forster, A. C.; Blacklow, S. C.; Cornish, V. W. *J. Am. Chem. Soc.* **2004**, *126*, 12752–12753. (c) Dedkova, L. M.; Fahmi, N. E.; Golovine, S. Y.; Hecht, S. M. *Biochemistry* **2006**, *45*, 15541–15551.
(5) (a) Goto, Y.; Ohta, A.; Sako, Y.; Yamagishi, Y.; Murakami, H.; Suga, H. *ACS Chem. Biol.* **2008**, *3*, 120–129. (b) Goto, Y.; Murakami, H.; Suga, H. *RNA* **2008**, *14*, 1390–1398.
(6) (a) Kozak, M. *Microbiol. Rev.* **1983**, *47*, 1–45. (b) Gold, L. *Annu. Rev. Biochem.* **1988**, *57*, 199–233. (c) Gualerzi, C. O.; Pon, C. L. *Biochemistry* **1990**, *29*, 5881–5889.
(7) Shimizu, Y.; Inoue, A.; Tomari, Y.; Suzuki, T.; Yokogawa, T.; Nishikawa, K.; Ueda, T. *Nat. Biotechnol.* **2001**, *19*, 751–755.
(8) (a) Ohta, A.; Murakami, H.; Higashimura, E.; Suga, H. *Chem. Biol.* **2007**, *14*, 1315–1322. (b) Sako, Y.; Goto, Y.; Murakami, H.; Suga, H. *ACS Chem. Biol.* **2008**, *3*, 241–249. (c) Sako, Y.; Morimoto, J.; Murakami, H.; Suga, H. *J. Am. Chem. Soc.* **2008**, *130*, 7232–7234. (d) Kawakami, T.; Murakami, H.; Suga, H. *Chem. Biol.* **2008**, *15*, 32–42.

JA900597D

nature
structural &
molecular biology

Bases in the anticodon loop of $tRNA^{Ala}_{GGC}$ prevent misreading

Hiroshi Murakami[1], Atsushi Ohta[2] & Hiroaki Suga[1,2]

The bases at positions 32 and 38 in the tRNA anticodon loop are known to have a specific conservation depending upon the anticodon triplets. Here we report that evolutionarily conserved pairs of bases at positions 32 and 38 in $tRNA^{Ala}_{GGC}$ prevent misreading of a near-cognate valine codon, GUC. The $tRNA^{Ala}_{GGC}$ molecules with the conserved A32-U38 and C32-G38 pairs do not read GUC, whereas those with three representative nonconserved pairs, U32-U38, U32-A38 and C32-A38, direct the misincorporation of alanine at this valine codon into the peptide chain. Overexpression of the nonconserved $tRNA^{Ala}_{GGC}$ in *Escherichia coli* is toxic and prevents cell growth. These results suggested that the bases at positions 32 and 38 in $tRNA^{Ala}_{GGC}$ evolved to preserve the fidelity of the cognate codon reading.

Decoding fidelity of translation relies on accurate selection of an aminoacyl-tRNA (aa-tRNA) whose anticodon base-pairs with the cognate codon encoded in the mRNA. It is well known that the third base pair in the codon-anticodon interaction tolerates a wobble pair represented by a U·G interaction, in addition to the canonical Watson-Click base pair, however, this decoding does not generally alter the identity of the amino acid in the peptide, and thus its fidelity is maintained[1]. On the other hand, if a U·G mispair at the first or second base pair occurs, such a codon-anticodon interaction does accompany an amino acid alteration, and therefore this kind of miscoding is generally prohibited. Still, some examples of misreading of the first codon have been reported in literature. For instance, in *Saccharomyces cerevisiae*, amber (UAG) mutations generated by UV irradiation are read by Gln-$tRNA^{Gln}_{CUG}$, causing termination to be suppressed by glutamine incorporation[2–6]. In *E. coli*, mutation of the AGC (serine) codon to GGC (glycine) codon at the catalytic Ser68 residue in β-lactamase is suppressed by the endogenous Ser-$tRNA^{Ser}_{GCU}$, although the probability of misreading resulting in glycine incorporation was estimated to be less than 1 in 1,000 (ref. 7).

It is also known that a base mutation or mutations near the junction of arms in the tRNA cloverleaf structure diminish decoding fidelity. One of the well-known cases is the G24A mutation in the D-stem of $tRNA^{Trp}_{CCA}$, the so-called Hirsh suppressor tRNA, which misreads CGG (arginine) and UGA (see **Fig. 1a** for a reference of the base position in a tRNA structure, $tRNA^{Ala}_{GGC}$)[8,9]. It was recently shown that the Hirsh suppressor $tRNA^{Trp}_{CCA}$ elevates the rates of both GTP hydrolysis and accommodation independently from the codon-anticodon interaction, and thus the misreading described above occurs[9]. These experiments suggest that, remotely, this base in the tRNA body has a crucial role in controlling the decoding event. Similarly, artificial mutations introduced into the C27-G43 Watson-Crick base pair in the anticodon stem of $tRNA^{Trp}_{CUG}$ increased the frequency of misreading of the first position wobble[10,11]. For instance, $tRNA^{Trp}_{CUG}$ bearing the G27-A43 mispair misread the UAG amber codon 40 times more frequently than the wild-type pair. Taken together with other biochemical data, it was postulated that such mutations possibly alter the angle of the junction of the anticodon stem and the central tRNA L-shaped structure, increasing the frequency of wobble reading[10].

Some bases in tRNA anticodon loop are also known to contribute to the maintenance of decoding fidelity. Although a typical example is base modifications in the anticodon loop that disrupt codon recognition[12,13], here we focus on sequence variations in the anticodon loop. For instance, *E. coli* has $tRNA^{Gly}$ with three isoacceptors for GGN (N can be any base) codons, whereas *Mycoplasma mycoides* has only $tRNA^{Gly}_{UCC}$ for reading these codons. It turns out that the difference in the sequence of the anticodon loop between *E. coli* $tRNA^{Gly}_{UCC}$ and *M. mycoides* $tRNA^{Gly}_{UCC}$ is a base at position 32, in which the former has U32 whereas the latter has C32, both pairing with A38. Notably, the U32C mutation introduced into *E. coli* $tRNA^{Gly}_{UCC}$ made it capable of reading all four glycine codons[14,15]. This suggests that the base at position 32 in the anticodon loop influences the tolerance of the U34·U and U34·C mispairs in codon-anticodon recognition. As described earlier, however, this misreading does not accompany an amino acid alteration. Hence, the study described above does not explain the importance of these bases at positions 32 and 38 in decoding fidelity. Nevertheless, this work prompted us to investigate whether the conservation of positions 32 and 38 contributes to the ability of tRNAs to correctly decode cognate codons in *E. coli*.

[1]Research Center for Advanced Science and Technology, University of Tokyo, Meguro-ku, Tokyo, Japan. [2]Department of Chemistry and Biotechnology, Graduate School of Engineering, University of Tokyo, Bunkyo-ku, Tokyo, Japan. Correspondence should be addressed to H.M. (hmura@rcast.u-tokyo.ac.jp) or H.S. (hsuga@rcast.u-tokyo.ac.jp).

Received 29 October 2008; accepted 13 February 2009; published online 22 March 2009; doi:10.1038/nsmb.1580

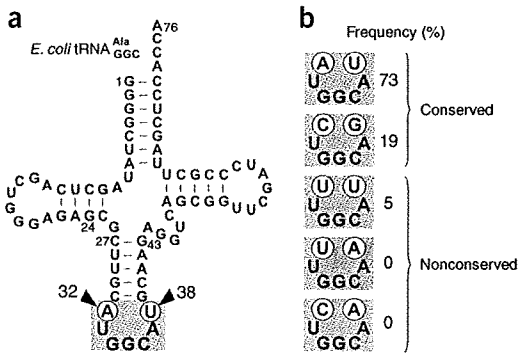

Figure 1 Structure of wild-type $tRNA^{Ala}_{GGC}$ and its variants (**a**) wild-type *E. coli* $tRNA^{Ala}_{GGC}$. (**b**) Frequency in the occurrence of the 32-38 pair in 84 nonredundant sequences of bacterial $tRNA^{Ala}_{GGC}$. The $tRNA^{Ala}_{GGC}$ with the A32-U38 and C32-G38 pairs are referred to as conserved $tRNA^{Ala}_{GGC}$, whereas those with the U32-U38, U32-A38 and C32-A38 pairs are referred to as nonconserved $tRNA^{Ala}_{GGC}$.

RESULTS

An evolutionary bias of the 32-38 pair in $tRNA^{Ala}_{GGC}$

First, we used the tDNA database to look for evolutionary bias in the 32-38 pair. Prior to our study, a 1982 report on the comparison of 42 kinds of *E. coli* and bacterial phage tRNA sequences focusing on the anticodon stem-loop region, proposed that some of the base pairs in the anticodon stem and the bases at positions 37 and 38 might show a preference for certain nucleotides depending upon the base at position 36, which forms the first base pair in the codon-anticodon interaction[16]. This finding has led to 'the extended anticodon hypothesis', which posits that these bases evolved to optimize translation efficiency and, possibly, decoding fidelity. Furthermore, this hypothesis was experimentally verified by suppression of the amber codon by mutant $tRNA^{Trp}_{CUA}$, and of the ochre codon by mutant $tRNA^{Glu}_{UUA}$, demonstrating that tRNAs with an extended anticodon sequence showed the highest suppression efficiency[17–20].

More recently, 5,601 bacterial tRNA sequences were extracted from the tDNA database and used to analyze the statistical conservation of bases at the 32 and 38 positions[21]. Certain tRNAs have a specific subset of combinations that differ from those of other tRNAs. For instance, 99% of $tRNA^{Ala}_{GGC}$ contain either A32-U38 (77%) or C32-G38 (22%), whereas the bases contained in bacterial tRNAs in general have frequencies of 52% for C32-A38, 17% for U32-A38, 11% for U32-U38 and 8% for C32-C38. Notably, $tRNA^{Ala}_{GGC}$ derivatives with nonconserved pairs such as U32-U38 and U32-A38 dissociate from the A site of the *E. coli* ribosome four to ten times more slowly than those containing A32-U38 (ref. 22). Moreover, the U32C mutation of $tRNA^{Gly}_{CCC}$, which is 98% conserved with the U32-A38 pair, increases the affinity of the tRNA not only to the cognate codon but also to the near-cognate codons involving third position mismatches[21]. These results imply that the 32-38 pair influences the affinity of tRNAs in the A site; however, again, these third position mismatches in the codon-anticodon interaction do not alter the amino acid, so it is unclear whether the evolutionary force driving this bias in the 32-38 pair, which depends on the anticodon triplet, arises from the need to control efficiency in translation or decoding fidelity.

We also independently searched the bacterial tDNA database[23] to assess the sequence bias in the 32-38 pair in 84 nonredundant sequences of bacterial $tRNA^{Ala}_{GGC}$. We found a trend similar to that previously described[21] (**Fig. 1**). Note that no bacterial $tRNA^{Ala}_{GGC}$ contains U32-A38 and C32-A38 pairs, whereas archeal $tRNA^{Ala}_{GGC}$ has the U32-A38 pair (18% out of 17 nonredundant sequences) but, again, no C32-A38 pair. Because the above sequence bias in the 32-38 pair possibly determines the translation efficiency of Ala-$tRNA^{Ala}_{GGC}$, we analyzed the difference in translation efficiency of *in vitro* transcripts between *E. coli* $tRNA^{Ala}_{GGC}$ (**Fig. 1a**) with the conserved A32-U38 pair (wild type) or the C32-G38 pair, as well as the nonconserved U32-U38, U32-A38 and C32-A38 pairs (**Fig. 1b**). For simplicity, we refer the former and latter sets of $tRNA^{Ala}_{GGC}$ as conserved and nonconserved $tRNA^{Ala}_{GGC}$, respectively.

No change in the decoding efficiency of the GCC cognate codon

To assess the translation efficiency of each $tRNA^{Ala}_{GGC}$ variant, we used an *E. coli* cell-free translation system that was specially reconstituted for this experiment. In this system, the native tRNAs were entirely substituted with *in vitro* transcripts of four tRNAs ($tRNA^{fMet}_{CAU}$, $tRNA^{Tyr}_{GUA}$, $tRNA^{Asp}_{GUC}$ and $tRNA^{Lys}_{CUU}$; we refer to the mixture of these tRNAs as 'tRNA mix') along with a $tRNA^{Ala}_{GGC}$, referred to as the *w*PURE system (w stands for 'withdrawn'). To validate whether this

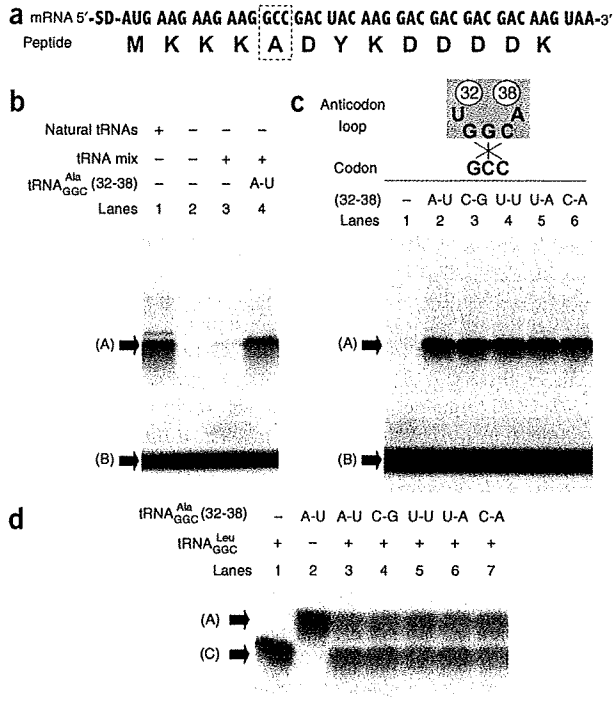

Figure 2 Decoding efficiency of the GCC codon by $tRNA^{Ala}_{GGC}$ with the conserved or nonconserved 32-38 pair. (**a**) Sequences of mRNA and peptide used in this study. The GCC (alanine) codon was placed at the fifth position. (**b**) Tricine SDS-PAGE analysis of the peptide expressed in the presence of tRNA mix and wild-type $tRNA^{Ala}_{GGC}$ in the *w*PURE system. The tRNA mix consists of *in vitro* transcripts of $tRNA^{fMet}_{CAU}$, $tRNA^{Tyr}_{GUA}$, $tRNA^{Asp}_{GUC}$ and $tRNA^{Lys}_{CUU}$. The peptide was expressed at 37 °C for 15 min in the presence of 0.2 mM proteinogenic amino acids (except aspartate) and 50 μM [^{14}C]aspartate. Arrows indicate alanine-containing peptide (A) and [^{14}C]aspartate (B). (**c**) Tricine SDS-PAGE analysis of the peptide in the presence of tRNA mix and each $tRNA^{Ala}_{GGC}$ variant in the *w*PURE system. (**d**) Tricine SDS-PAGE analysis of the competitive decoding of the GCC codon by Ala-$tRNA^{Ala}_{GGC}$ and Leu-$tRNA^{Leu}_{GGC}$ in the *w*PURE system. The competition contained 3 μM $tRNA^{Leu}_{GGC}$ and each $tRNA^{Ala}_{GGC}$ variant to a concentration of 3 μM. Arrows indicate Ala-peptide (A) and Leu-peptide (C).

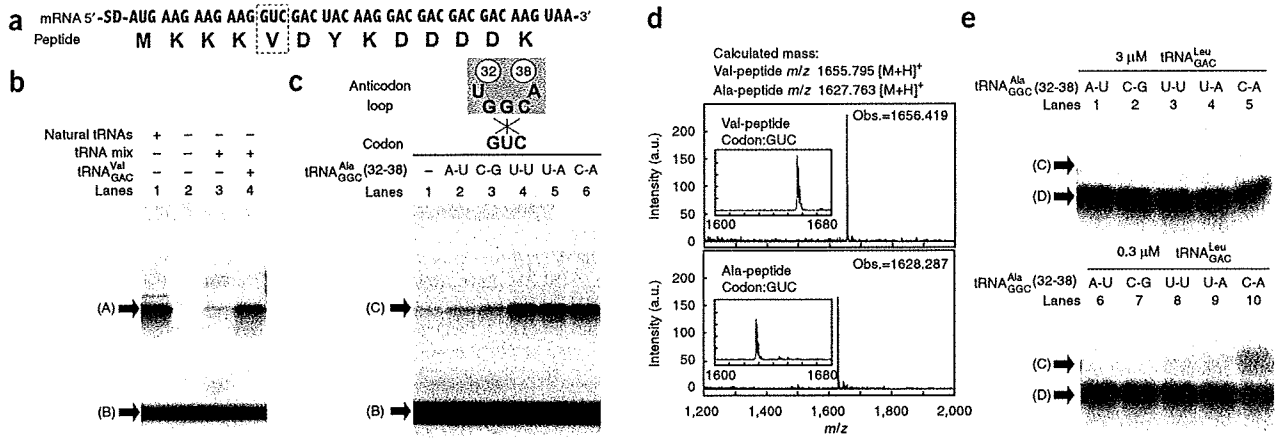

Figure 3 Influence of the sequence variation of the 32-38 pair in tRNA$^{Ala}_{GGC}$ on misreading of GUC codon. (**a**) Sequences of mRNA and peptide used in this study. The GUC (valine) codon was placed at the fifth position. (**b**) Tricine SDS-PAGE analysis of the peptide expressed in the presence of tRNA mix and the *in vitro* transcript of tRNA$^{Val}_{GAC}$ in the *w*PURE system. Other conditions were the same as **Figure 2b**. Arrows indicate Val-peptide (A) and [^{14}C]aspartate (B). (**c**) Tricine SDS-PAGE analysis of the peptide in the presence of tRNA mix and each tRNA$^{Ala}_{GGC}$ variant in the *w*PURE system. Arrows indicate Ala-peptide (C) (and Val-peptide in lane 1) and [^{14}C]aspartate (B). (**d**) MALDI-TOF analysis of the peptides expressed above. The Val-peptide (codon: GUC) was obtained from the expression sample in lane 4 in **Figure 3b** with aspartate instead of [^{14}C]aspartate. The Ala-peptide (codon: GUC) was obtained from the expression sample in lane 6 in **Figure 3c** with aspartate instead of [^{14}C]aspartate. Inset, expansion of the region between 1,600 and 1,680 *m/z* of the MS spectra. (**e**) Competitive decoding of the GUC codon by tRNA$^{Ala}_{GGC}$ variants and tRNA$^{Leu}_{GAC}$. In lanes 1–5, 3 μM tRNA$^{Leu}_{GAC}$ and 3 μM each tRNA$^{Ala}_{GGC}$ variant were used; in lanes 6–10, 0.3 μM tRNA$^{Leu}_{GAC}$ and 3 μM each tRNA$^{Ala}_{GGC}$ variant were used. Arrows indicate Ala-peptide (C), Leu-peptide (D).

*w*PURE system was able to function like the ordinary PURE system[24] for the expression of a model peptide consisting of amino acids assigned by the above tRNAs, a 13-mer peptide, MKKKA*DYKDDDDK* (italicized residues indicate a Flag peptide sequence), was expressed from the corresponding mRNA (**Fig. 2a**) in the presence of wild-type tRNA$^{Ala}_{GGC}$ and [^{14}C]Asp in both systems. We determined the expression level of the peptide by the intensity of the radioactive band following tricine SDS-PAGE, showing that the *w*PURE system functioned like the ordinary PURE system for the expression of this peptide (**Fig. 2b**, lane 1 versus lane 4). Most importantly, the expression was tRNA$^{Ala}_{GGC}$ dependent (lanes 3 and 4). MALDI-TOF analysis of the peptide expressed in the *w*PURE system also confirmed the accuracy of expression (data not shown), indicating that correct reading of the GCC codon could be achieved by tRNA$^{Ala}_{GGC}$.

We then tested the tRNA$^{Ala}_{GGC}$ variants (**Fig. 1**) in the *w*PURE system for the decoding ability of the respective tRNAs to the GCC cognate codon. It should be noted that because *E. coli* alanyl-tRNA synthetase (AlaRS) does not recognize the anticodon loop[25–27], all the tRNA$^{Ala}_{GGC}$ variants were alanylated by AlaRS with virtually the same efficiency (**Supplementary Fig. 1** online). Thus, the observed translation efficiency is likely to reflect the intrinsic decoding ability of each tRNA$^{Ala}_{GGC}$ to the GCC codon. Unexpectedly, we observed no difference in incorporation efficiency (**Fig. 2c**).

To avoid exhausting the energy source of translation, we terminated the reaction described above after 15 min (**Supplementary Fig. 2** online); however, it was still possible that the difference in the decoding ability of each tRNA$^{Ala}_{GGC}$ was so small that the apparent translation efficiency was not sensitive enough to reflect to the actual value under such conditions. We therefore performed an additional experiment to rule out this possibility. Because *E. coli* leucinyl-tRNA synthetase (LeuRS) does not recognize the anticodon loop of tRNA^{Leu} (refs. 28–30), LeuRS charged leucine on the engineered tRNA^{Leu} carrying the anticodon loop sequence of *E. coli* wild-type tRNA$^{Ala}_{GGC}$ (**Supplementary Figs. 1** and **3** online). In fact, when we added tRNA$^{Leu}_{GGC}$ to the *w*PURE system instead of tRNA$^{Ala}_{GGC}$, translation of the same mRNA took place smoothly (**Fig. 2d**, lane 1). Notably, this leucine-containing peptide (Leu-peptide) appeared as a faster-migrating band than the alanine-containing peptide (Ala-peptide) band in tricine SDS-PAGE (**Fig. 2d**, lanes 1 and 2). MALDI-TOF analysis also revealed a molecular mass consistent with the Leu-peptide (data not shown), indicating that the single substitution of alanine to leucine in this peptide altered its migration properties. Thus, this feature allowed us to use tricine SDS-PAGE to conveniently assess the expression level of the individual peptides in competition assays between tRNA$^{Ala}_{GGC}$ and tRNA$^{Leu}_{GGC}$. We observed no appreciable difference in the intensities between the Ala- and Leu-peptides generated by any of tRNA$^{Ala}_{GGC}$ variants competing with tRNA$^{Leu}_{GGC}$ (lanes 3–7). These experiments clearly showed that the conserved and nonconserved tRNA$^{Ala}_{GGC}$ variants were able to decode the GCC cognate codon with similar efficiencies. We thus suspected that the evolutionary conservation of the 32-38 pair in tRNA$^{Ala}_{GGC}$ arose for a different reason(s).

The 32-38 pair controls misreading of GUC near-cognate codon

As sequence variation in the 32-38 pair did not affect decoding efficiency, we turned our investigation toward its decoding fidelity. The wobble pairing at the second G35 in tRNA$^{Ala}_{GGC}$ to a near-cognate valine codon, GUC, would be expected to alter the amino acid incorporation from valine to alanine. We therefore prepared another mRNA template based on the previously used mRNA in which the GCC codon was substituted with a GUC codon, and tested whether misreading by tRNA$^{Ala}_{GGC}$ would result in this substitution (**Fig. 3a**).

We first monitored the background incorporation of valine into the GUC codon in the *w*PURE system, which lacks the *in vitro* transcripts. In the absence of the tRNA mix, mRNA translation did not occur at all (**Fig. 3b**, lane 2); however, addition of the tRNA mix stimulated the expression of peptide (**Fig. 3b**, lane 3). Even though the isolated background-level peptide was present only in trace amounts, MALDI-TOF analysis revealed that it was consistent with the molecular mass

of the valine-containing peptide (Val-peptide) as a major peak (data not shown). This suggests that the background expression can be attributed to a trace amount of $tRNA^{Val}_{GAC}$ contaminating the *w*PURE system. On the other hand, addition of the *in vitro* transcript of $tRNA^{Val}_{GAC}$ to the *w*PURE system markedly elevated the expression level of peptide (**Fig. 3b**, lane 4).

We then tested whether alanine misincorporation at the GUC codon could be induced by addition of $tRNA^{Ala}_{GGC}$ variants to the *w*PURE system. The presence of wild-type or C32-G38 $tRNA^{Ala}_{GGC}$ slightly increased the background expression, presumably owing to misreading of the GUC codon resulting in alanine incorporation into the peptide chain (**Fig. 3c**, lanes 1–3). Unexpectedly, the presence of nonconserved $tRNA^{Ala}_{GGC}$ (U32-U38, U32-A38 and C32-A38) substantially increased the expression level (**Fig. 3c**, lanes 4–6, respectively). MALDI-TOF analysis of the isolated peptide showed a single major peak of molecular mass corresponding to the Ala-peptide (**Fig. 3d**). This result clearly shows that the background incorporation at the GUC codon by the contaminated $tRNA^{Val}_{GAC}$ was completely competed out by the nonconserved $tRNA^{Ala}_{GGC}$.

Even though the nonconserved $tRNA^{Ala}_{GGC}$ misreads GUC effectively in the *w*PURE system, in *E. coli* the cognate $tRNA^{Val}_{GAC}$ coexists endogenously and thus competes out such a misreading event. Therefore, it was necessary to assess how effectively misreading occurred under the competitive conditions. Because the Val-peptide and the Ala-peptide had nearly the same migration pattern in tricine SDS-PAGE (**Fig. 3b,c**), it was difficult to quantitatively assess the competition. Instead, we engineered a $tRNA^{Leu}$ containing the native anticodon loop sequence of *E. coli* $tRNA^{Val}_{GAC}$ (**Supplementary Fig. 3c**) and used it as a competitor against each $tRNA^{Ala}_{GGC}$ variant. As expected on the basis of previous experiments[28–30], LeuRS charged leucine onto the engineered $tRNA^{Leu}_{GAC}$ (**Supplementary Fig. 1**) and the resulting Leu-$tRNA^{Leu}_{GAC}$ decoded the mRNA GUC codon, yielding the Leu-peptide. Because the Leu-peptide migrated faster than the Ala-peptide in tricine-SDS-PAGE, we could readily visualize the degree of competition (**Fig. 3e**).

When we added an equal amount of each $tRNA^{Ala}_{GGC}$ variant and $tRNA^{Leu}_{GAC}$ to the *w*PURE system, only the Leu-peptide band was observed in all cases, suggesting that each Ala-$tRNA^{Ala}_{GGC}$ variant was completely competed out by Leu-$tRNA^{Leu}_{GAC}$ (**Fig. 3e**, lanes 1–5). However, when we reduced the concentration of the $tRNA^{Leu}_{GAC}$ to one-tenth that of $tRNA^{Ala}_{GGC}$, a faint but clearly visible Ala-peptide band appeared in the presence of the nonconserved $tRNA^{Ala}_{GGC}$ (**Fig. 3e**, lanes 6–10). Particularly, the frequency of misreading of GUC by Ala-$tRNA^{Ala}_{GGC}$ containing the C32-A38 pair reached approximately 30% (**Fig. 3e**, lane 10). This result clearly indicates that the 32-38 pair in $tRNA^{Ala}_{GGC}$ controls misreading of the near-cognate GUC codon.

Overexpression of the nonconserved $tRNA^{Ala}_{GGC}$ is toxic in *E. coli*

The above *in vitro* experiments clearly demonstrated that the nonconserved $tRNA^{Ala}_{GGC}$ misreads the near-cognate GUC codon involving the G35·U wobble pair. We wondered whether this misreading event could occur *in vivo*, so that the nonconserved $tRNA^{Ala}_{GGC}$ acts as a toxigenic tRNA. We transformed *E. coli* BL21 cells with a vector that could overexpress each conserved or nonconserved $tRNA^{Ala}_{GGC}$ variant under the control of an arabinose promoter (**Supplementary Fig. 4** online). The tranformed cells were grown individually on either 0.2% (w/v) glucose (negative control) or 0.2% (w/v) arabinose on LB agar plates at 42 °C. Before induction of tRNA expression, all cells appeared as healthy as the untransformed control cells (**Fig. 4a**). Upon induction, cells expressing the conserved $tRNA^{Ala}_{GGC}$ showed no change in growth, whereas those expressing the nonconserved $tRNA^{Ala}_{GGC}$ became

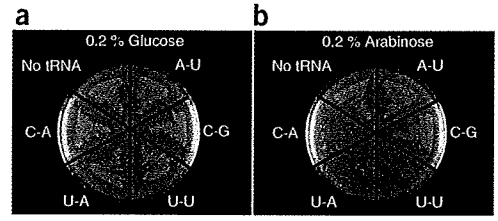

Figure 4 Overexpression of the conserved or nonconserved $tRNA^{Ala}_{GGC}$ in *E. coli* (BL21). Each $tRNA^{Ala}_{GGC}$ variant was cloned under the control of the arabinose promoter. LB plates contained 100 μg ml^{-1} ampicillin in the presence of 0.2% (w/v) glucose (**a**) or 0.2% (w/v) arabinose (**b**) and were incubated at 42 °C overnight.

unhealthy (**Fig. 4b**). Particularly, those expressing the nonconserved $tRNA^{Ala}_{GGC}$ with U32-A38 or C32-A38 were unable to grow. These U32-A38 and C32-A38 pairs were never found in the $tRNA^{Ala}_{GGC}$ sequence database, indicating that the sequence bias of the 32-38 pair in $tRNA^{Ala}_{GGC}$ probably appeared to avoid formation of toxigenic tRNAs *in vivo*.

It should be noted that at 37 °C most cells appeared to be healthy, with the exception of those cells expressing the nonconserved $tRNA^{Ala}_{GGC}$ with C32-A38, which grew slightly more slowly (data not shown). This temperature sensitivity may suggest that the frequency of the misreading of the GUC codon by $tRNA^{Ala}_{GGC}$ with the nonconserved C32-A38 pair is not marked because the codon is predominantly read correctly by the cognate $tRNA^{Val}_{GAC}$. However, in some proteins the resulting valine to alanine substitution would cause them to be less stable, resulting in loss of function at 42 °C. This probably led to the observed temperature-dependent cell growth. Nonetheless, our demonstration clearly shows that the nonconserved $tRNA^{Ala}_{GGC}$ is toxic *in vivo* and is therefore not conserved in the repertoire of functional tRNAs.

DISCUSSION

Here we provide *in vitro* evidence that the nonconserved $tRNA^{Ala}_{GGC}$ (**Fig. 1**) misreads its near-cognate valine codon, GUC, resulting in misincorporation of alanine into the valine site of the peptide chain (**Fig. 3**). In contrast, misreading of this codon by the conserved $tRNA^{Ala}_{GGC}$ (**Fig. 1**) is minimal and thus is readily competed out by the cognate $tRNA^{Leu}_{GAC}$ (**Fig. 3**). This observation is also valid *in vivo*, where overexpression of the nonconserved $tRNA^{Ala}_{GGC}$ is toxic, whereas that of the conserved $tRNA^{Ala}_{GGC}$ is not (**Fig. 4**). These results imply that the reason for the evolutionary force selecting the 32-38 pair in $tRNA^{Ala}_{GGC}$ is to secure the decoding fidelity.

Fidelity of aa-tRNA selection in the ribosome relies on two mechanistic steps, so-called initial selection and proofreading, which occur before and after GTP hydrolysis, respectively[31,32]. In the initial selection step, incorrect tRNA is rejected by rapid dissociation of the ternary complex of aa-tRNA–EF-Tu–GTP from the A site and the sluggish rate of GTP hydrolysis[33,34]. Even though GTP hydrolysis occasionally occurs for the incorrect aa-tRNA, in the next proofreading step the slow accommodation rate of the incorrect aa-tRNA to the peptidyl-transferase center results in its rejection, and therefore incorrect reading of the noncognate codon is avoided[34]. It is likely that the sequence variation of 32-38 pair in $tRNA^{Ala}_{GGC}$ also influences either or both steps of aa-tRNA selection. It was reported that the nonconserved $tRNA^{Ala}_{GGC}$(U32-U38 or U32-A38) binding to the cognate GCC codon has a slower dissociation rate from the A site than the conserved $tRNA^{Ala}_{GGC}$(A32-U38 or C32-G38)[22]. Therefore, an

explanation for the increase in the frequency of misreading of GUC by such nonconserved $tRNA^{Ala}_{GGC}$ is also due to their slow dissociation rate from the ribosome. Recently, various kinetics measurements were performed for misreading of near-cognate codons, including GUC, by the conserved $tRNA^{Ala}_{GGC}$(A32-U38, C32-G38) and non-conserved $tRNA^{Ala}_{GGC}$(U32-A38 or C32-A38)[35]. The apparent rate of peptide bond formation in misreading of the GUC codon by the two nonconserved $tRNA^{Ala}_{GGC}$(U32-A38 or C32-A38) is elevated to the level of that which occurs during reading of the cognate GCC codon. Clearly, this result is consistent with our finding that the nonconserved $tRNA^{Ala}_{GGC}$ tends to misread the near-cognate GUC codon.

Structures of the anticodon loop with various 32-38 pairs have been modeled *in silico* based on the available crystal structures[36]. The U32-A38 and C32-A38 pairs, belonging to the largest structural family I, form noncanonical structures involving bifurcated hydrogen bonds. In contrast, the U32-U38 pair, categorized in family II, forms a single, noncanonical hydrogen bond. Structures for the A32-U38 and C32-G38 pairs, in family III, cannot yet be predicted because of insufficient available structural information. It should be noted that families I and II combined constitute about 93% of bacterial tRNAs[36], implying that these base pairs evolved to maximize the decoding ability of tRNAs on the ribosome. In the present study, we have shown that, paradoxically, the family I $tRNA^{Ala}_{GGC}$ with U32-A38 or C32-A38 and the family II $tRNA^{Ala}_{GGC}$ with U32-U38 misread GUC codon. Consequently, the rare family III pairs, A32-U38 and C32-G38, are found in the naturally occurring $tRNA^{Ala}_{GGC}$. This suggests that the decoding fidelity of $tRNA^{Ala}_{GGC}$ is tuned by selecting uncommon 32-38 pairs during the evolution. Presumably, similar unique sequence biases that tune decoding fidelity can be found in many regions of the tRNA body sequence[37]. More extensive sequence analyses of tRNAs and biochemical studies on such evolutionarily biased variants will be important to reveal the mechanism of decoding fidelity in translation.

METHODS

Materials. We prepared all of the tRNAs by *in vitro* run-off transcription using T7 RNA polymerase[38], and the DNA templates of mRNAs (5′-CGAAG CTAAT ACGAC TCACT ATAGG GCTTT AATAA GGAGA AAAAC ATGAA GAAGA AGNNN GACTA CAAGG ACGAC GACGA CAAGT AAGCT TCG -3′, where NNN indicates GCC or GUC, and the underlined sequence encodes the T7 promoter) by PCR using *Taq* DNA polymerase (**Supplementary Methods** online).

Translation. We performed batch translation using the PURE system without the tRNA mixture (*w*PURE system) according to described protocols[39–42]. The translation mixture contained 50 mM HEPES-K^+, pH 7.6, 20 mM creatine phosphate, 100 mM potassium glutamate, 14 mM magnesium acetate, 2 mM EDTA, 2 mM spermidine, 1 mM DTT, 2 mM ATP, 2 mM GTP, 1 mM UTP, 1 mM CTP and 10 μM 10-formyl-5,6,7,8-tetrahydrofolic acid. The translation was carried out with 0.02 μM DNA template of mRNA and a 200 μM concentration of 19 kinds of proteinogenic amino acids without aspartate and 50 μM [^{14}C]Asp. Natural tRNA extract (1.5 mg ml^{-1} at final concentration, Roche) was added in the control experiment. *In vitro* transcripts of $tRNA^{fMet}$, $tRNA^{Tyr}$, $tRNA^{Asp}$ (5 μM each tRNA at final concentration) and $tRNA^{Lys}$ (40 μM at final concentration) were added instead of natural tRNA extract in other all experiments. The concentrations of $tRNA^{Ala}_{GGC}$ variants, $tRNA^{Val}_{GAC}$, the engineered $tRNA^{Leu}_{GGC}$ and $tRNA^{Leu}_{GAC}$ are described in the figures. The reaction was carried out in a total volume of 2 μl at 37 °C for 15 min and the products were analyzed by tricine SDS-PAGE.

Mass spectroscopy measurements of peptides. For MS analysis, we performed the reactions (5 μl) with a 200 μM concentration of 20 proteinogenic amino acids. The products were precipitated with 50 μl of acetone, dissolved in 2.5 μl of water and then immobilized with 2.5 μl of Flag–M2 agarose (Sigma). After the resin was washed twice with 50 μl of W buffer (50 mM Tris-HCl, pH 8.0, 150 mM NaCl), the immobilized peptides were eluted with 2.5 μl of 0.2% (v/v) trifluoroacetic acid (TFA), desalted with Zip tips C18 (Millipore) and eluted with 1.5 μl of a 50% (v/v) acetonitrile, 0.1% (v/v) TFA solution saturated with the matrix (*R*)-cyano-4-hydroxycinnamic acid. Mass measurements were performed using MALDI-TOF (Autoflex, Bruker) in the positive mode and externally calibrated with Substance P (average 1,348.66 Da), Bombesin (average 1,620.88 Da), ACTH clip 1–17 (average 2,094.46 Da) and Somatostatin 28 (average 3,149.61 Da) as standards.

Construction of plasmids. The DNA fragment was amplified by *Pyrobest* DNA polymerase (Takara) from pUC18 using primers (pUCHin.F33, 5′-GCAAG CTTGC TCTTC CGCTT CCTCG CTCAC TGA-3′, and pUCNotPst.R44, 5′-CCGCT GCAGA CGCGG CCGCG CCTGA TGCGG TATTT TCTCC TTAC-3′) and the product was digested with PstI and HindIII. The annealed DNA fragment (5′-GATCC TTAGC GAAAG CTAAG GATTT TTTTT A-3′ and 5′-AGCTT AAAAA AAATC CTTAG CTTTC GCTAA GGATC TGCA-3′) containing rrnC terminator was cloned in the PstI–HindIII site of the product DNA. The resulting plasmid was named pMUC. The DNA region that contains the *araC* gene and the P_{BAD} promoter of pBAD–GFPuv (BioRad) was amplified by PCR using primers (araNot.F35, 5′-ACGCG GCCGC GCATA ATGTG CCTGT CAAAT GGACG-3′, and araEcoPst.R43, 5′-CCGCT GCAGC AGAAT TCCCA AAAAA ACGGG TATGG AGAAA CAG-3′). After NotI-PstI digestion, the fragment was cloned into the NotI-PstI site of pMUC. The resulting plasmid was named pMUCA. Template DNA of $tRNA^{Ala}_{GGC}$ variants were amplified using primers (EcoT7.F26, 5′-GCGAA TTCTA ATACG ACTCA CTATA G-3′, and AlaPst.R35, 5′-GCGCT GCAGT GTTAT TGGTG GAGCT AAGCG GGATC-3′) from the corresponding PCR products described above and digested with EcoRI and PstI, and then cloned into EcoRI-PstI site in pMUCA. We confirmed the sequence between NotI-HindIII site by sequence analysis.

Overexpression of the $tRNA^{Ala}_{GGC}$ variant in *E. coli*. The plasmids were transformed into BL21 (Invitrogen) and spread on LB agar plates containing 100 mg ml^{-1} ampicillin and 4% (w/v) glucose. The plates were incubated at 37 °C overnight and the colonies were cultivated in LB medium containing 100 μg ml^{-1} ampicillin and 4% (w/v) glucose at 37 °C overnight. The cultures were diluted by 10× volume of LB medium and streaked on LB agar plates containing 100 μg ml^{-1} amplicillin and 0.2% (w/v) glucose or 0.2% (w/v) arabinose. The plates were incubated at 42 °C overnight.

Note: Supplementary information is available on the Nature Structural & Molecular Biology website.

ACKNOWLEDGMENTS

We thank O.C. Uhlenbeck and S. Ledoux for their invaluable discussion. This work was supported by grants from the Japan Society for the Promotion of Science (JSPS) Grants-in-Aid for Scientific Research (S) (16101007) to H.S., a Young Scientists (A) (20681022) to H.M., a JSPS Fellowship (19-1722) to A.O., a research and development project of the Industrial Science and Technology Program in the New Energy and Industrial Technology Development Organization (NEDO) to H.S., the Industrial Technology Research Grant Program in NEDO (05A02513a) to H.M., and the Takeda Science Foundation.

AUTHOR CONTRIBUTIONS

This study was designed by H.M., A.O. and H.S.; all of the experiments were performed by H.M.; the paper was written by H.M. and H.S.

Published online at http://www.nature.com/nsmb/
Reprints and permissions information is available online at http://npg.nature.com/reprintsandpermissions/

1. Crick, F.H. Codon–anticodon pairing: the wobble hypothesis. *J. Mol. Biol.* **19**, 548–555 (1966).
2. Calderon, I.L., Contopoulou, C.R. & Mortimer, R.K. Isolation of a DNA fragment that is expressed as an amber suppressor when present in high copy number in yeast. *Gene* **29**, 69–76 (1984).
3. Pure, G.A., Robinson, G.W., Naumovski, L. & Friedberg, E.C. Partial suppression of an ochre mutation in *Saccharomyces cerevisiae* by multicopy plasmids containing a normal yeast $tRNA^{Gln}$ gene. *J. Mol. Biol.* **183**, 31–42 (1985).
4. Lin, J.P., Aker, M., Sitney, K.C. & Mortimer, R.K. First position wobble in codon-anticodon pairing: amber suppression by a yeast glutamine tRNA. *Gene* **49**, 383–388 (1986).

5. Weiss, W.A. & Friedberg, E.C. Normal yeast $tRNA^{Gln}_{CAG}$ can suppress amber codons and is encoded by an essential gene. *J. Mol. Biol.* **192**, 725–735 (1986).
6. Weiss, W.A., Edelman, I., Culbertson, M.R. & Friedberg, E.C. Physiological levels of normal $tRNA^{Gln}_{CAG}$ can effect partial suppression of amber mutations in the yeast *Saccharomyces cerevisiae*. *Proc. Natl. Acad. Sci. USA* **84**, 8031–8034 (1987).
7. Toth, M.J., Murgola, E.J. & Schimmel, P. Evidence for a unique first position codon-anticodon mismatch *in vivo*. *J. Mol. Biol.* **201**, 451–454 (1988).
8. Hirsh, D. Tryptophan transfer RNA as the UGA suppressor. *J. Mol. Biol.* **58**, 439–458 (1971).
9. Cochella, L. & Green, R. An active role for tRNA in decoding beyond codon:anticodon pairing. *Science* **308**, 1178–1180 (2005).
10. Schultz, D.W. & Yarus, M. tRNA structure and ribosomal function. I. tRNA nucleotide 27–43 mutations enhance first position wobble. *J. Mol. Biol.* **235**, 1381–1394 (1994).
11. Schultz, D.W. & Yarus, M. tRNA structure and ribosomal function. II. Interaction between anticodon helix and other tRNA mutations. *J. Mol. Biol.* **235**, 1395–1405 (1994).
12. Takai, K. & Yokoyama, S. Roles of 5-substituents of tRNA wobble uridines in the recognition of purine-ending codons. *Nucleic Acids Res.* **31**, 6383–6391 (2003).
13. Agris, P.F., Vendeix, F.A. & Graham, W.D. tRNA's wobble decoding of the genome: 40 years of modification. *J. Mol. Biol.* **366**, 1–13 (2007).
14. Lustig, F. *et al.* Codon discrimination and anticodon structural context. *Proc. Natl. Acad. Sci. USA* **86**, 6873–6877 (1989).
15. Lustig, F. *et al.* The nucleotide in position 32 of the tRNA anticodon loop determines ability of anticodon UCC to discriminate among glycine codons. *Proc. Natl. Acad. Sci. USA* **90**, 3343–3347 (1993).
16. Yarus, M. Translational efficiency of transfer RNA's: uses of an extended anticodon. *Science* **218**, 646–652 (1982).
17. Raftery, L.A. & Yarus, M. Site-specific mutagenesis of *Escherichia coli* gltT yields a weak, glutamic acid-inserting ochre suppressor. *J. Mol. Biol.* **184**, 343–345 (1985).
18. Yarus, M., Cline, S.W., Wier, P., Breeden, L. & Thompson, R.C. Actions of the anticodon arm in translation on the phenotypes of RNA mutants. *J. Mol. Biol.* **192**, 235–255 (1986).
19. Raftery, L.A. & Yarus, M. Systematic alterations in the anticodon arm make $tRNA^{Glu}$-Suoc a more efficient suppressor. *EMBO J.* **6**, 1499–1506 (1987).
20. Smith, D., Breeden, L., Farrell, E. & Yarus, M. The bases of the tRNA anticodon loop are independent by genetic criteria. *Nucleic Acids Res.* **15**, 4669–4686 (1987).
21. Olejniczak, M. & Uhlenbeck, O.C. tRNA residues that have coevolved with their anticodon to ensure uniform and accurate codon recognition. *Biochimie* **88**, 943–950 (2006).
22. Olejniczak, M., Dale, T., Fahlman, R.P. & Uhlenbeck, O.C. Idiosyncratic tuning of tRNAs to achieve uniform ribosome binding. *Nat. Struct. Mol. Biol.* **12**, 788–793 (2005).
23. Sprinzl, M., Horn, C., Brown, M., Ioudovitch, A. & Steinberg, S. Compilation of tRNA sequences and sequences of tRNA genes. *Nucleic Acids Res.* **26**, 148–153 (1998).
24. Shimizu, Y. *et al.* Cell-free translation reconstituted with purified components. *Nat. Biotechnol.* **19**, 751–755 (2001).
25. Hou, Y.M. & Schimmel, P. A simple structural feature is a major determinant of the identity of a transfer RNA. *Nature* **333**, 140–145 (1988).
26. Francklyn, C. & Schimmel, P. Aminoacylation of RNA minihelices with alanine. *Nature* **337**, 478–481 (1989).
27. Tamura, K., Asahara, H., Himeno, H., Hasegawa, T. & Shimizu, M. Identity elements of *Escherichia coli* $tRNA^{Ala}$. *J. Mol. Recognit.* **4**, 129–132 (1991).
28. Normanly, J., Ogden, R.C., Horvath, S.J. & Abelson, J. Changing the identity of a transfer RNA. *Nature* **321**, 213–219 (1986).
29. Asahara, H. *et al.* Recognition nucleotides of *Escherichia coli* $tRNA^{Leu}$ and its elements facilitating discrimination from $tRNA^{Ser}$ and $tRNA^{Tyr}$. *J. Mol. Biol.* **231**, 219–229 (1993).
30. Tukalo, M., Yaremchuk, A., Fukunaga, R., Yokoyama, S. & Cusack, S. The crystal structure of leucyl-tRNA synthetase complexed with $tRNA^{Leu}$ in the post-transfer-editing conformation. *Nat. Struct. Mol. Biol.* **12**, 923–930 (2005).
31. Rodnina, M.V. & Wintermeyer, W. Fidelity of aminoacyl-tRNA selection on the ribosome: kinetic and structural mechanisms. *Annu. Rev. Biochem.* **70**, 415–435 (2001).
32. Rodnina, M.V. & Wintermeyer, W. Ribosome fidelity: tRNA discrimination, proofreading and induced fit. *Trends Biochem. Sci.* **26**, 124–130 (2001).
33. Pape, T., Wintermeyer, W. & Rodnina, M.V. Complete kinetic mechanism of elongation factor Tu-dependent binding of aminoacyl-tRNA to the A site of the *E. coli* ribosome. *EMBO J.* **17**, 7490–7497 (1998).
34. Pape, T., Wintermeyer, W. & Rodnina, M. Induced fit in initial selection and proofreading of aminoacyl-tRNA on the ribosome. *EMBO J.* **18**, 3800–3807 (1999).
35. Ledoux, S., Olejniczak, M. & Uhlenbeck, O.C. A sequence element that tunes *Escherichia coli* $tRNA^{Ala}_{GGC}$ to ensure accurate decoding. *Nat. Struct. Mol. Biol.* advance online publication, doi:10.1038/nsmb.1581 (22 March 2009).
36. Auffinger, P. & Westhof, E. Singly and bifurcated hydrogen-bonded base-pairs in tRNA anticodon hairpins and ribozymes. *J. Mol. Biol.* **292**, 467–483 (1999).
37. Saks, M.E. & Conery, J.S. Anticodon-dependent conservation of bacterial tRNA gene sequences. *RNA* **13**, 651–660 (2007).
38. Milligan, J.F., Groebe, D.R., Witherell, G.W. & Uhlenbeck, O.C. Oligoribonucleotide synthesis using T7 RNA polymerase and synthetic DNA templates. *Nucleic Acids Res.* **15**, 8783–8798 (1987).
39. Shimizu, Y., Kanamori, T. & Ueda, T. Protein synthesis by pure translation systems. *Methods* **36**, 299–304 (2005).
40. Goto, Y. *et al.* Reprogramming the translation initiation for the synthesis of physiologically stable cyclic peptides. *ACS Chem. Biol.* **3**, 120–129 (2008).
41. Kawakami, T., Murakami, H. & Suga, H. Messenger RNA-programmed incorporation of multiple N-methyl-amino acids into linear and cyclic peptides. *Chem. Biol.* **15**, 32–42 (2008).
42. Sako, Y., Goto, Y., Murakami, H. & Suga, H. Ribosomal synthesis of peptidase-resistant peptides closed by a nonreducible inter-side-chain bond. *ACS Chem. Biol.* **3**, 241–249 (2008).

Biochemical and Biophysical Research Communications 381 (2009) 533–536

Contents lists available at ScienceDirect

Biochemical and Biophysical Research Communications

journal homepage: www.elsevier.com/locate/ybbrc

TRAIL inhibited the cyclic AMP responsible element mediated gene expression

Yasuhito Tokumoto [a,*], Katsuhisa Horimoto [b], Jun Miyake [a,c]

[a] Department of Bioengineering, Graduate School of Engineering, The University of Tokyo, 7-3-1 Hongo, Bunkyo-ku, Tokyo 113-8656, Japan
[b] Computational Biology Research Center (CBRC), National Institute of Advanced Industrial Science and Technology (AIST), 2-42 Aomi, Koto-ku, Tokyo135-0064, Japan
[c] Research Institute for Cell Engineering (RICE), National Institute of Advanced Industrial Science and Technology (AIST), 1-8-31 Midorigaoka, Ikeda, Osaka 563-8577, Japan

ARTICLE INFO

Article history:
Received 14 February 2009
Available online 20 February 2009

Keywords:
CRE
CREB
TRAIL
Signal transduction
Transcription

ABSTRACT

Tumor necrosis factor (TNF)-related apoptosis-inducing ligand (TRAIL) not only causes apoptotic cell death in tumor cells, but also activates some transcription factors and affects several other cellular functions. In this study, we observed the effect of administration of TRAIL on gene expression downstream of the cyclic AMP responsive element (CRE) enhancer by using the signal transduction reporter *cis*-element plasmid pCRE-d2EGFP. Western blotting showed that after administration of TRAIL, the expression level of reporter protein d2EGFP was down-regulated in NIH3T3 cells. To confirm the TRAIL-induced down-regulation of CRE enhancer controlled gene expression, DNA Chip time series analysis of the intrinsic genes expressed in NIH3T3 cells was carried out. As a result, the expression levels of six genes, which have CRE sequence in their promoter region, were slightly down-regulated within three hours after administration of TRAIL.

Introduction

Tumor necrosis factor (TNF)-related apoptosis-inducing ligand (TRAIL) is a member of the structurally related TNF cytokine family [1,2]. TRAIL has apoptotic anticancer activity which is not accompanied by general toxicity in most normal cells and tissues. Unfortunately, the mechanism of this tumor specific toxicity is unknown. TRAIL binds to death receptors (DR4 or DR5), which are expressed on their target cell surface, as trimers. The binding of a TRAIL trimer is followed by a trimer formation of DRs and aggregation of Fas-associated death domain (FADD) and procaspase-8 to the cytoplasmic region of DRs. The complex of these molecules is called the death inducing signal complex (DISC). In DISC, procaspase-8 is digested to become the activated caspase-8 that is the initiator of the apoptotic caspase cascade. In addition to this proteolytic cascade, the TRAIL-DR complex also activates transcription factors via TNF receptor type 1 associated death domain protein (TRADD) to the TNF receptor-associated factor 2 (TRAF2) pathway [1]. The activation of nuclear factor kappa B (NF-κB) and c-Jun (cellular oncogene ju-nana) by TRAF2 is well established. Under TRAIL stimulation, activated NF-κB induces the transcription of the genes of the cellular form of Fas-associated death domain like interleukin-1beta-converting enzyme inhibitory protein (cFLIP) and inhibitor of apoptosis protein (IPA); both proteins inhibit caspase-8. Compared with NF-κB, the function of c-Jun in TRAIL stimulation is more controversial. Moderate and long-term activation of c-Jun is pro-apoptotic, but strong and short-term activation of c-Jun is anti-apoptotic [2].

Recently, two independent groups reported that cAMP-responsive element binding protein (CREB), another transcription factor, is also phosphorylated by TRAIL stimulation [3,4]. CREB was initially identified as a target of the cyclic AMP (cAMP) signaling pathway, but studies on the activation of the immediate early genes revealed that CREB is a substrate for other than cAMP-dependent protein kinase A [5]. All signaling pathways that activate CREB lead to the phosphorylation of a particular residue, serine 133 (Ser133). Phosphorylated CREB specifically binds to the genomic DNA at a conserved cAMP-responsive element (CRE), which consists of an eight-base pair palindrome (TGACGTCA) and is typically found within 100 nucleotides from the TATA box [6,7]. Phosphorylated CREB also recruits another nuclear protein, CREB-binding protein (CBP). After binding to phosphorylated CREB, CBP serves as a molecular bridge that allows upstream transcription factors to recruit and stabilize the RNA polymerase II transcription complex at the TATA box. Although TRAIL-dependent phosphorylation of CREB has been shown in two tumor cell lines, SK-N-MC (neuroblastoma) and Jurkat (T cell leukemia), both are TRAIL sensitive and die within a few hours after administration of TRAIL, so it was difficult to identify the target genes of the phosphorylated CREB. In this study, we search for target genes of phosphorylated CREB after TRAIL stimulation in the TRAIL-resistant non-tumor cell line NIH3T3 [8]. First, by using the CRE containing signal transduction reporter plasmid pCRE-d2EGFP, we estimated the transcriptional activity of CREB by western blotting. Second, by a DNA Chip time series analysis, we evaluated the effect of TRAIL administration on the gene

* Corresponding author. Fax: +81 3 5841 1792.
E-mail address: y.tokumoto@will.dpc.u-tokyo.ac.jp (Y. Tokumoto).

0006-291X/$ - see front matter © 2009 Elsevier Inc. All rights reserved.
doi:10.1016/j.bbrc.2009.02.076

expression patterns of the intrinsic genes, which possess CRE sequences in their promoter regions.

Materials and methods

Materials. All chemicals without annotation were purchased from Wako Pure Chemical Industries. Dulbecco's modified Eagle's medium (DMEM), Opti-MEM1, Lipofectamine 2000, fetal bovine serum (FBS), Trypsin–EDTA, Antibiotic–Antimycotic mixture (penicillin, streptomycin, amphotericin B) were purchased from Invitrogen. Soybean trypsin inhibitor and Complete Mini proteinase inhibitor mix were purchased from Roche. 25 cm^2 Tissue culture flasks (T25) and 6 well cell culture plates were purchased from Nunc. Twenty-four well glass bottom culture plate (EzView) was purchased from Asahi Techno Glass. Cell strainer (40 mm nylon mesh) was purchase from Becton–Dickinson. Human recombinant TRAIL was purchased from PeproTech EC. Forskolin was purchased from Sigma–Aldrich.

Transfection of reporter plasmid to NIH3T3. The destabilized fluorescence protein d2EGFP gene containing signal transduction *cis*-element repoter plasmid pCRE-d2EGFP DNA (Clontech, #6034-1) and the control plasmid pd2EGFP-N1 DNA (Clontech, #6009-1) were purchased from Clontech. Plasmid DNA purification was carried out by using EndoFree Plasmid Maxi kit (QIAGEN #12362). Mouse embryonic fibroblast cell line NIH3T3 (RCB 1862) was provided by RIKEN Bio-Resource Center (Ibaraki, Japan). Cells were cultured in DMEM-10% FBS at 37 °C in 5% CO_2. Transfection was carried out by using a Lipofectamine 2000 transfection reagent according to the supplier's instruction. In short, for 3.0×10^6 cells of NIH3T3 inoculated in T25 culture flask, 12 μg plasmid DNA and 30 μl of Lipofectamine 2000 transfection reagent mixture diluted in 1.5 ml of OPTI-MEM1 was added over night. The transfection efficiency was examined by using an Olympus IX 70 fluorescence inverted microscope.

Western blotting. NIH3T3 pCRE-d2EGFP transient transfectant cells and NIH3T3 pd2EGFP-N1 transient transfectant cells were inoculated in the 6 well cell culture plate (2.0×10^6 cells/well in 3 ml of DMEM-10% FBS). Cells were cultured over night at 37 °C in 5% CO_2. After then they were treated with TRAIL (200 ng/ml) or forskolin (10 μM). Harvest of the cells was carried out every hour. Cells were washed twice by ice-cold PBS and lysed in 100 μl of RIPA buffer (50 mM Tris–HCl, pH 7.5, 150 mM NaCl, 1% NP40, 0.5% sodium deoxycholate, 10 mM EDTA) containing Complete Mini proteinase inhibitor mix. The protein concentration of each crude extract was estimated by using BCR protein assay kit (PIERCE) according to the supplier's instructions. Ten micrograms of protein containing each samples loaded on individual well of 10% polyacrylamide gel and SDS–PAGE was carried out. After the electrophoresis, proteins were electro-transferred to Immun-blot PVDF membrane (Bio-Rad). After blocking by skim milk, PVDF membrane blotted with rabbit polyclonal anti-GFP antibody (MBL) for 1 h. Membrane was washed three times by PBS-T, then the second antibody, HRP conjugated goat anti-rabbit IgG antibody (Cell Signaling) was added. Existing chemiluminescent detection was carried out by using an ECL plus western blotting detection system (GE Healthcare). The pattern of blotting on PVDF membrane was imaged by a Typhoon 9410 Variable Mode Imager (GE Healthcare). The intensity of each band was estimated by ImageQuant TL software (GE Healthcare). For the internal control assay, the PVDF membrane was stripped by Restore PLUS western Blot Stripping Buffer (Thermo Scientific). The blocking procedure was carried out again and followed by the blotting of mouse monoclonal anti-β-tubulin antibody and HRP conjugated goat anti-mouse Ig polyclonal antibody (GE Healthcare).

DNA Chip time series analysis. NIH3T3 pCRE-d2EGFP transient transfectant cells were inoculated in the 6 well cell culture plate (2.0×10^6 cells/well in 3 ml of DMEM-10% FBS). Cells were cultured over night at 37 °C in 5% CO_2. After then they were treated with TRAIL (200 ng/ml) and harvested at 0, 1, 2, 3 h after the administration of TRAIL. They were washed twice with ice-cold PBS. The preparations of total RNA were carried out by using the RNeasy Plus Mini kit (QIAGEN). After the estimation of the quality and the quantity, 10 μg of total RNA of each sample was used for Affymetrix Mouse gene 1.0 ST Array assay (Affymetrix). Array data were analyzed by using the GeneSpring GX 7.3.1 software (Affymetrix).

Results and discussion

For the assay of TRAIL-induced CREB activation, we used the signal transduction *cis*-element reporter plasmid pCRE-d2EGFP. This plasmid contains three copies of the CRE enhancer consensus sequence (TGACGTCA) fused to a TATA-like promoter region from the Herpes simplex virus thymidine kinase promoter. In this system the activation of CREB, which binds to CRE, induces transcription of d2EGFP mRNA. After transfection of pCRE-d2EGFP into NIH3T3, we administrated TRAIL (200 ng/ml) and observed cell death and expression of d2EGFP using fluorescence microscopy. During a 24-h period, NIH3T3/pCRE-d2EGFP cells did not show either the cell death or an apparent increase in fluorescence of the d2EGFP protein (data not shown). It is said that the slow rate of chromophore formation and the stability of EGFP preclude the use of EGFP as a reporter to monitor fast changes in promoter activity [9,10]. To solve this problem, we tried to use a destabilized form of EGFP, d2EGFP, as a reporter protein, but it did not work well.

Since the cell biological assay might not suitable for this experiment, we tried to evaluate the protein expression level of d2EGFP by western blotting, a biochemical assay. First 200 ng/ml of TRAIL was administered to NIH3T3/pCRE-d2EGFP transient transfectant cells. At that time, for the positive control of CREB–CRE transcriptional activation, these cells were also treated with 10 μM of forskolin [11]. The cells were harvested every hour and the time-course samples were assessed by western blotting. The result was contrary to expectations. As shown in Fig. 1, the expression level of the reporter protein d2EGFP in NIH3T3 was clearly down-regulated from 4 h after administration of TRAIL. Because the d2EGFP protein increased from 8 h after administration of forskolin (positive control), the CREB–CRE transcription activation system worked well in NIH3T3 cells. Quantitative analysis showed that after 10 h of TRAIL administration, the amount of d2EGFP de-

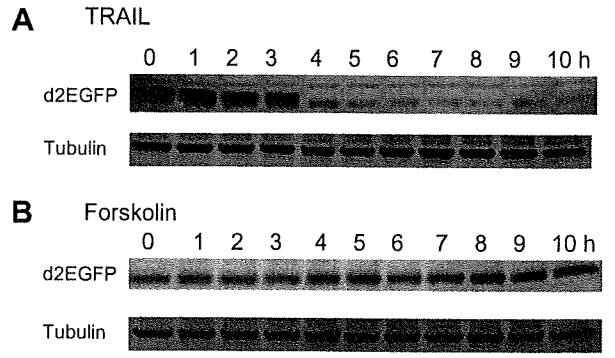

Fig. 1. A time-course analysis of reporter protein d2EGFP expression in NIH3T3 cells by western blotting. NIH3T3 cells harboring pCRE-d2EGFP plasmid DNA were treated by TRAIL (200 ng/ml) or forskolin (10 μM) and harvested every hour (0–10 h). (A) TRAIL-treated cells. (B) Forskolin-treated cells. The upper panel is anti-GFP antibody blotting (d2EGFP) and the lower panel is anti-β-tubulin antibody blotting (tubulin, as an internal control).

creased to less than 5% (Fig. 2). It was possible that the TRAIL-activated proteolysis cascade (caspase-8, caspase-3) might preferentially degrade d2EGFP protein. Therefore we transfected pd2EGFP-N1 plasmid DNA into NIH3T3 cells and used them in the TRAIL administration experiment. pd2EGFP-N1 is a cell-labeling plasmid containing a d2EGFP gene driven by the CMV promoter. NIH3T3 cells harboring pd2EGFP-N1 plasmid DNA constitutively expressed d2EGFP protein without any stimulation. As shown in Fig. 3, the administration of TRAIL to pd2EGFP-N1 transfected NIH3T3 cells did not reduce the amount of d2EGFP protein, so the hypothesis of accelerated degradation of d2EGFP protein was disproved.

To observe if this TRAIL-induced transcriptional inhibition downstream of the CRE enhancer occured only in the ex-chromosomal transient gene expression system or not, we examined the NIH3T3 cells' intrinsic gene expression pattern after administration of TRAIL by an exhaustive DNA Chip analysis. The reporter protein d2EGFP is a destabilized variant of the EGFP protein, and its half-life is around 2 h in a mammalian cell [9]. Because the down-regulation of d2EGFP protein in NIH3T3 cells occurred at 4 h after administration of TRAIL (Fig. 1), we estimated that the inhibition of the gene transcription of d2EGFP had to happen within 3 h after administration of TRAIL. Thus our study was focused on this time period. In previous studies, 23 genes were confirmed as being under the control of the CREB–CRE system [6,7]. Depending on the DNA Chip analysis data, we examined the transcription level of these genes from 1 to 3 h after administration of TRAIL (Table 1). Although six genes (26%) were down-regulated, but only one gene (4%) was up-regulated. The other 16 genes (70%) were unaffected. These data showed that TRAIL signaling works as a repressor of the CREB–CRE transcription system in NIH3T3 cells.

In previous studies, two independent groups reported the TRAIL induces phosphorylation of CREB at its Ser133. However the phosphorylation of CREB did not always elevate its transcriptional activity. Ca^{2+}/calmodulin-dependent protein kinase type II (CaMKII) is a member of the calmodulin serine/threonine kinase family. CaMKII phosphorylates CREB at its two of serine residues, one being the authentic Ser133, and the other Ser142. Phosphorylation of Ser142 inhibits the CREB transcriptional activity even when Ser133 is phosphorylated [12,13].

It is worth noting that the only gene that was up-regulated by TRAIL stimulation was c-fos (Gene ID 14281). c-Fos is a transcription factor that forms the heterodimer complex AP-1 with c-Jun [14]. As described previously, c-Jun is the major player in TRAIL-induced transcriptional control. Therefore the up-regulation of c-fos transcription may contribute to the resistance of NIH3T3 against TRAIL-induced apoptosis.

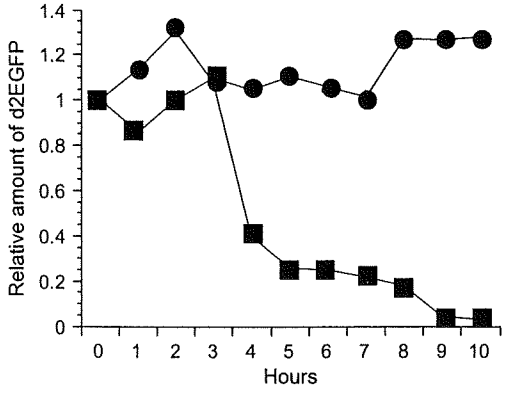

Fig. 2. Quantitative analysis of the band intensity of the western blots shown in Fig. 1. The intensity of each band was estimated by ImageQuant TL software and normalized by the band intensity of tubulin (internal control) in the same lane. The expression level of the d2EGFP protein is shown as the relative amount against time 0. Closed squares represent TRAIL-stimulated cells and closed circles represent forskolin-stimulated cells.

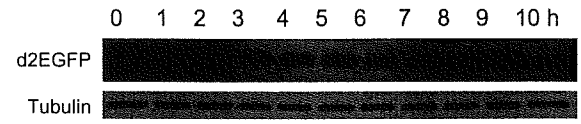

Fig. 3. TRAIL did not affect the stability of the d2EGFP protein. NIH3T3 cells harboring pd2EGFP-N1 plasmid DNA were treated by TRAIL (200 ng/ml) and harvested every hour (0–10 h). Western blotting was carried out. The upper panel is anti-GFP antibody blotting (d2EGFP) and the lower panel is anti-β-tubulin antibody blotting (tubulin, as an internal control).

Table 1
The effect of TRAIL administration to the intrinsic gene expressions.

Name	Gene ID	Time 0	1 h	2 h	3 h
Cryaa	12954	1	0.900	0.913	0.796
Cyp19a1	13075	1	0.945	0.884	0.842
Penk1	18619	1	0.771	0.968	0.724
Pth	19226	1	0.806	0.917	0.893
Polb	18970	1	0.915	0.848	0.819
Tat	234724	1	0.780	0.752	0.708
Fos	14281	1	1.133	1.157	1.216
Adrb2	11555	1	1.064	1.054	1.035
Chgb	12653	1	1.070	0.966	0.968
Cycs	13063	1	0.844	1.039	0.968
Fn1	14268	1	0.962	0.958	0.966
Gcg	14526	1	0.985	0.935	0.960
Hsd11b1	15483	1	0.930	1.084	1.198
H2-D1	14964	1	0.951	1.022	0.997
Ldha	16828	1	1.054	0.988	1.023
Pck1	18534	1	1.130	1.133	0.946
Plau	18792	1	0.876	0.915	0.967
Pou1f1	18736	1	0.925	0.944	0.914
Scg2	20254	1	0.929	0.991	0.917
Sst	20604	1	0.928	0.879	1.023
Syn1	20964	1	1.054	0.953	1.079
Th	21823	1	0.967	0.951	1.045
Vip	22353	1	1.018	0.991	0.944

The genes listed above possess at least one CRE site that is required for CREB-binding in their promoter region (6, 7). Relative amount of their transcripts after the TRAIL administration (0–3 h) estimated by DNA chip analysis was shown.

Acknowledgments

This study was supported by a project grant from New Energy and Industrial Technology Development Organization (NEDO; Japan). We thanks to Qiaofan Li and Shinpei Tamaki for their technical supports.

References

[1] F.C. Kimberley, G.R. Screaton, Following a TRAIL: update on a ligand and its five receptors, Cell Res. 14 (2004) 359–372.
[2] C. Falschlehner, C.H. Emmerich, B. Gerlach, H. Walczak, TRAIL signaling: decisions between life and death, Int. J. Biochem. Cell Biol. 39 (2007) 1462–1475.
[3] D. Milani, G. Zauli, E. Rimondi, C. Celeghini, S. Marmiroli, P. Narducci, S. Capitani, P. Secchiero, Tumor necrosis factor-related apoptosis-inducing ligand sequentially activates pro-survival and pro-apoptotic pathways in SK-N-MC neuronal cells, J. Neurochem. 86 (2003) 126–135.
[4] L. Caravatta, S. Sancilio, V. Di Giacomo, R. Rana, A. Cataldi, R. Di Pietro, PI3-K/AKT-dependent activation of cAMP-response element-binding (CREB) protein in Jurkat T Leukemia cells treated with TRAIL, J. Cell. Physiol. 214 (2008) 192–200.
[5] A.J. Shaywitz, M.E. Greenberg, CREB: a stimulus-induced transcription factor activated by a diverse array of extracellular signals, Annu. Rev. Biochem. 68 (1999) 821–861.
[6] M. Montminy, Transcriptional regulation by cyclic AMP, Annu. Rev. Biochem. 66 (1997) 807–822.

[7] K.A.W. Lee, N. Masson, Transcriptional regulation by CREB and its relatives, Biochim. Biophys. Acta 1174 (1993) 221–233.
[8] B.J. Kim, M.-S. Kim, K.-B. Kim, K.-W. Kim, Y.-M. Hong, I.-K. Kim, H.-W. Lee, Y.-K. Jung, Sensitizing effects of cadmium on TNF-α-and TRAIL-mediated apoptosis of NIH3T3 cells with distinct expression pattern of p53, Carcinogenesis 23 (2002) 1411–1417.
[9] R. Heim, D.C. Prasher, R.Y. Tsien, Wavelength mutations and posttranslational autoxidation of green fluorescent protein, Proc. Natl. Acad. Sci. USA 91 (1994) 12501–12504.
[10] I. Davis, C.H. Girdham, P.H. O'Farrell, A nuclear GFP that marks nuclei in living *Drosophila* embryos; maternal supply overcomes a delay in the appearance of zygotic fluorescence, Dev. Biol. 170 (1995) 726–729.
[11] K.B. Seamon, W. Padgett, J.W. Daly, Forskolin: unique diterpene activator of adenylate cyclase in membrane and in intact cells, Proc. Natl. Acad. Sci. USA 78 (1981) 3363–3367.
[12] P.K. Dash, K.A. Karl, M.A. Colicos, R. Prywes, E.R. Kandel, CAMP response element-binding protein is activated by Ca^{2+}/calmodulin- as well as cAMP-dependent protein kinase, Proc. Natl. Acad. Sci. USA 88 (1991) 5061–5065.
[13] P. Sun, H. Enslen, P.S. Myung, Differential activation of CREB by Ca^{2+}/calmodulin-dependent protein kinases type II and type IV involves phosphorylation of a site that negatively regulates activity, Genes Dev. 8 (1994) 2527–2539.
[14] L.A. Tibbles, J.R. Woodgett, The stress-activated protein kinase pathways, Cell. Mol. Life Sci. 55 (1999) 1230–1254.